Observations of Nonequilibrium Electrical Discharge in an MHD Disk Generator

Nobuhiro Harada,* Hiroyuki Yamasaki,† and Susumu Shioda‡
Tokyo Institute of Technology, Yokohama, Japan

Nonequilibrium discharge phenomena in an MHD disk generator with potassium-seeded argon as a working gas have been investigated experimentally using a shock tube facility. A detailed study of high-speed photographs shows that an unsteady motion of a strongly constricted discharge occurs, particularly in the disk entrance region, characterized by a negative Hall potential. Responding to a suitable external load resistance, the negative Hall potential is reduced due to the development of a stable region against the ionization instability under full seed ionization; thus, a substantial increase output of power can be achieved. Under this condition, a uniform discharge is observed downstream and the strongly inhomogeneous and unsteady discharge is confined to a narrow region at the entrance. For smaller load resistances, intense spiral arcs with enhanced fluctuations are observed.

Introduction

In a magnetohydrodynamic (MHD) generator, the transport properties of the plasma are strongly influenced by the spatial nonuniformity of the electrical discharge. Especially in a seeded nonequilibrium inert gas, the nonuniformity of the discharge is generally enhanced due to the strong coupling between the electrical conductivity and the Joule heating of the electrons. This nonuniformity causes a decrease in the effective values of the electrical conductivity and Hall parameter and, therefore, leads to a decrease in generator performance.[1,2] It also affects the MHD interaction between the Lorentz force and a flowfield. Under high-interaction conditions with substantial enthalpy extraction, gasdynamical shock occurs by local enhancement of the Lorentz force due to a constricted discharge that imposes a limit on the performance of an MHD generator.[3,4] It is, therefore, important to maintain a uniform discharge in an MHD generator.

Previous experiments using a simulated linear MHD channel with applied external voltage[5-8] have shown that when a magnetic field is applied, the discharge is concentrated in nonstationary streamers due to the ionization instability[9] (or electrothermal instability[10]), resulting in the reduction of the effective electrical conductivity and Hall parameter. Thus, much effort has been made to suppress the ionization instability. Stabilization of the ionization instability is achieved experimentally by completely ionizing the seed under conditions of a low seed fraction.[11,12] At the same time, this fact is expected to keep the unsteady concentration of the discharge confined to the entrance region of the linear channel, which means that the effect of this unsteady concentration of the discharge is reduced downstream.[12]

These experiments have been carried out with an externally applied voltage. Under power generating conditions, the experimental results with a disk Hall generator[13] and a linear Faraday generator[14] have shown that suppressing the ionization instability under the condition of a fully ionized seed results in a recovery of the effective Hall parameter and output power. Furthermore, almost complete recovery of the effective values of electrical conductivity and Hall parameter is achieved.[15,16] However, the discharge structure under these conditions has not been clarified.

In the present paper, the results of high-speed photographic observation of the discharge structure in a nonequilibrium MHD disk generator under power generating conditions are described.

Experimental Arrangements and Measurements

The experimental setup of the shock tube facility is shown in Fig. 1. Argon gas is passed through the potassium seed tank, which is heated by a burner at the bottom. Then the gas mixture is introduced continuously into the driven section of the shock tube and is pumped out by a rotary vacuum pump in front of the diaphragm. This provides a steady flow of the gas mixture throughout the driven section, as well as a homogeneous mixing of the argon and potassium. The seed fraction is controlled by adjusting the temperature of the seed tank and the flow rate of the carrier argon gas on the basis of the attenuation of the potassium resonance line intensity, which is monitored at the driven section before rupture of the shock tube diaphragm.

A schematic view of the MHD generator Disk-II that was used in these experiments is shown in Fig. 2. This figure also shows the optical system used for the high-speed camera observations. The inner and outer radii of the disk channel are 10.3 and 16.3 cm, respectively. The cross-sectional area of the disk channel is constant (100 cm^2) along the flow direction to give a constant ideal Hall parameter throughout the channel.

One of the insulating walls of Disk-II channel is equipped with eight cylindrical stainless steel probes in order to monitor the electric potential profile and its fluctuations. The Hall voltage measured by these electric probes is isolated by a photoisolated amplifier. Six optical fiber and static pressure ports are also provided in the disk channel to detect the potassium resonance line intensity, its fluctuations, and its static pressure distribution. The locations of these electric probes and measuring ports are indicated in Fig. 2. Measured signals are recorded by using a 12 channel digital wave memory and an 8 channel oscilloscope systems whose frequency responses are up to 100 kHz.

The iron core magnet, which is excited by a d.c. power supply, can provide the maximum magnetic field strength of 1.53 T. But in the present experiments, the magnetic induction is reduced to 1.24 T since the gap between the pole pieces of the magnet core had to be increased in order to prepare a space outside of the generator insulating wall for a high-speed camera measurement system. An image converter camera,

Received May 10, 1985; revision received Nov. 20, 1985.

*Research Associate, Department of Energy Sciences.
†Associate Professor, Department of Energy Sciences.
‡Professor, Department of Energy Sciences.

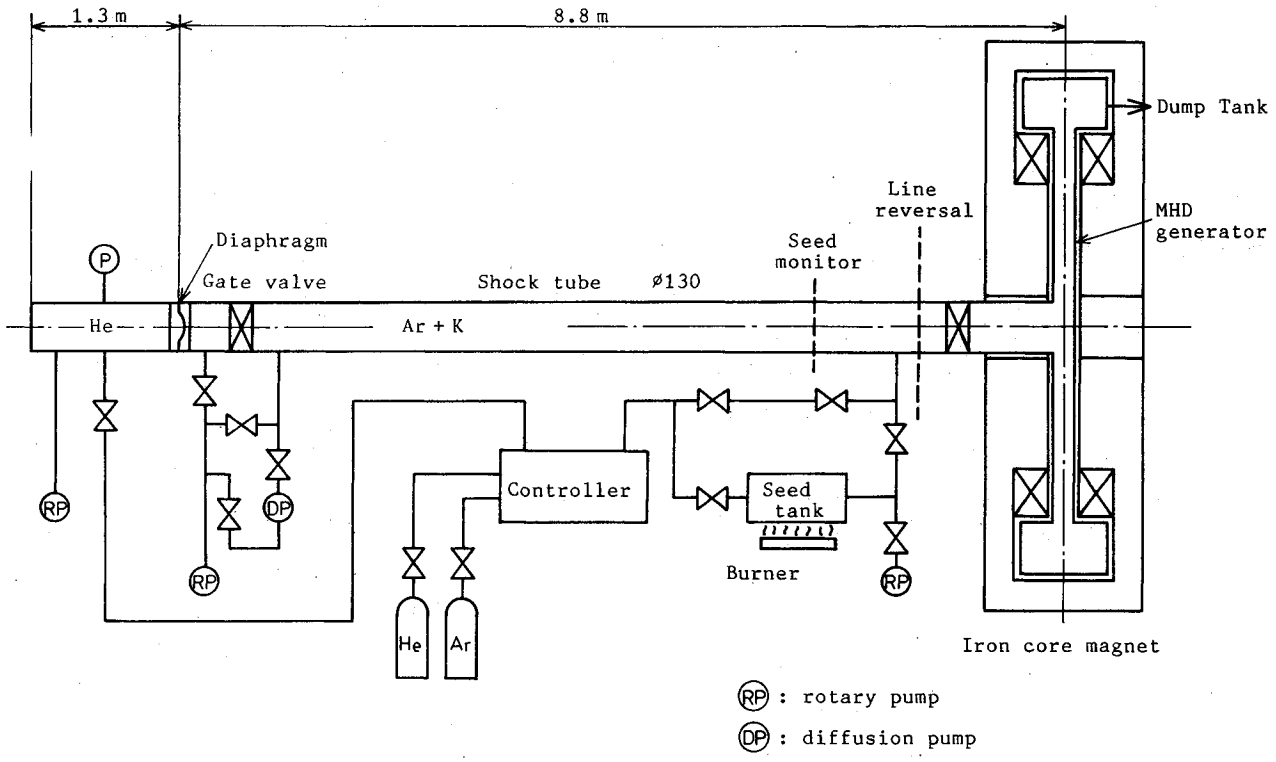

Fig. 1 Experimental setup of the shock tube.

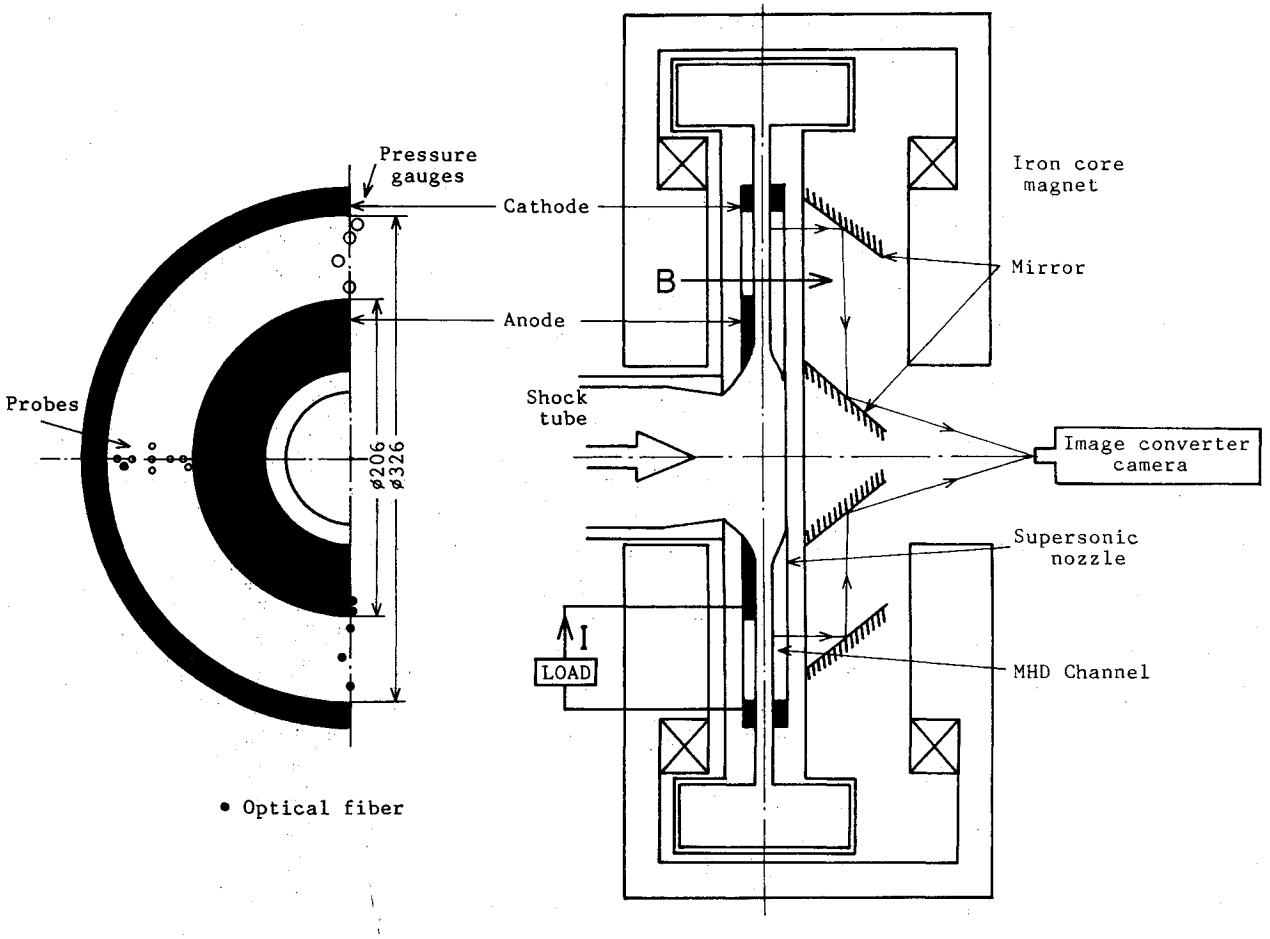

Fig. 2 Disk-II generator and the optical system for high-speed observations.

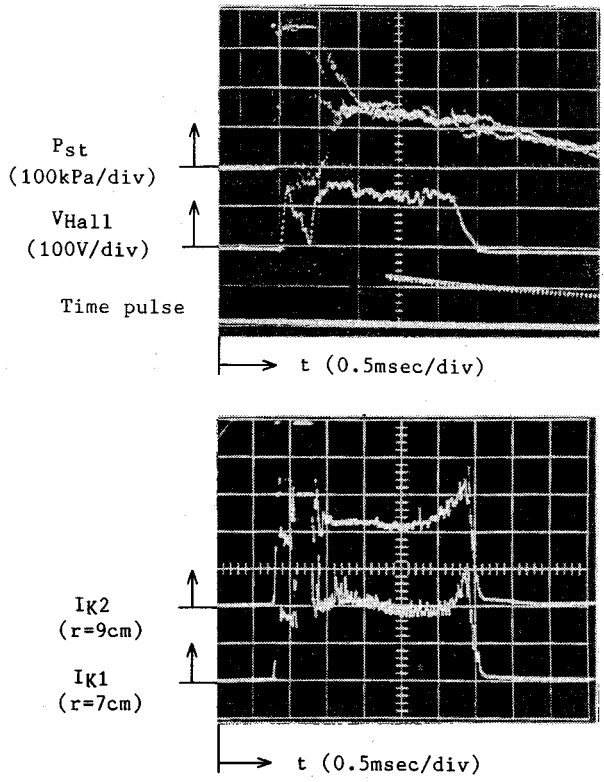

Fig. 3 Typical oscilloscope traces of stagnant pressure P_{st}, Hall voltage V_{Hall}, time pulse and potassium resonance line (4p-4s transition) intensity I_K1, I_K2.

Table Experimental conditions

Dimension of the channel	
Inner radius	10.3 cm
Outer radius	16.3 cm
Cross-sectional area	100 cm^2
Volume of the channel	600 cm^3
Working gas	Ar+K
Stagnant gas temperature	2500 K
Stagnant gas pressure	128 kPa
Mach number	2.3
Static gas temperature	905 K
Static gas pressure	10.1 kPa
Flow velocity	1288 m/s
Seed fraction	2.4×10^{-4}
Magnetic field strength	1.24 T

which can be operated in both framing and streak modes is used to photograph the discharge structure in the disk channel. Typical exposure time and typical frame interval for framing pictures are 1 and 5 μs, respectively. Since the gas velocity is about 1 mm/μs, the working gas can be considered stationary during the 1 μs exposure time. Typical duration time for streak pictures is 75 μs.

Experimental conditions are summarized in Table 1. The stagnant gas temperature is 2500 K and the seed fraction is 2.4×10^{-4} in order to obtain sufficient radiative intensity from the plasma for the high-speed camera in a short exposure time.

Experimental Results

Experiments were carried out by changing the external load from 0.05 to 1 kΩ to learn the generator performance and the discharge structure for various loading conditions.

The typical oscilloscope traces of the stagnation pressure signal, Hall voltage, and potassium resonance line intensity are shown in Fig. 3. In this figure, the time pulse for triggering the image converter camera is also shown. It can be seen that

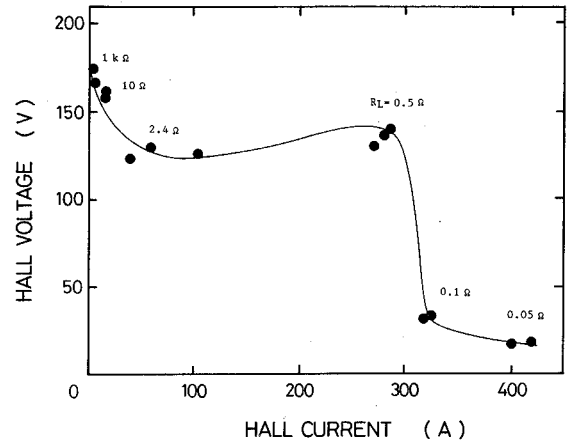

Fig. 4 Hall voltage/Hall current characteristic.

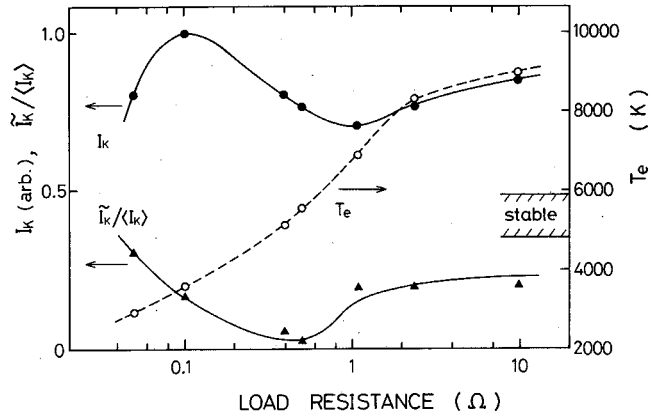

Fig. 5 Potassium resonance line (4p-4s transition) intensity I_K, its fluctuation $\tilde{I}_K/<I_K>$ and estimated electron temperature T_e.

the duration of power generation is about 1.7 ms following the transient state of 0.5 ms. The fluctuation of the pressure signal is caused by the oscillation of the sensor diaphragm.

Hall Voltage/Hall Current Characteristic

The Hall voltage/Hall current characteristic is shown in Fig. 4. It can be seen from this figure that the output power is recovered significantly for a load resistance of 0.5 Ω, where the seed becomes fully ionized and the ionization instability is much reduced. In this case, the output power has a value of 40 kW and the corresponding output power density is 67 MW/m^3.

Complete ionization of seed can be assured from the results shown in Fig. 5, in which the potassium resonance line intensity and its fluctuation level measured at $r = 14$ cm are plotted against the load resistances. This figure, also shows the electron temperature, estimated from relative intensity of the resonance line, and the stable regime of electron temperature against the ionization instability, which is derived from the linear perturbation theory.[11] We can see that the resonance line intensity decreases with the increase of load resistance from 0.1 to 1 Ω. This decrease in intensity is due to the decrease in the potassium neutral atom concentration as the seed becomes fully ionized. For the load resistance of 0.5 Ω, the fluctuations in the resonance line intensity almost disappear and the estimated electron temperature lies in the stable regime. When the load resistance falls below 0.1 Ω, the partially ionized potassium region prevails in the disk channel. In the case of electron temperatures above 7000 K for load resistances higher than 1 Ω, as is estimated from the measured potassium resonance line intensity, a situation in which the

argon becomes ionized in most of the disk channel is observed. Reduction of induced Hall voltage for load resistances above 1 Ω (see Fig. 4) can possibly be explained by the effects of the argon ionization instability and flow deceleration due to a strong Lorentz force.

Hall Potential Distribution

The Hall potential distribution is measured along the flow direction and the results are shown in Fig. 6. For lower load resistances, the negative potential region near the anode becomes significant. In this negative potential region, the voltage drop due to the internal resistance of the plasma becomes large as compared to the Hall electromotive force and, therefore, a part of the electric power generated downstream is consumed. This negative potential region becomes narrower with the increase in the external load, which indicates a increase in the electron Joule heating of the Hall generator.

For a external load resistance of 0.5 Ω, the negative potential region is confined to a relatively narrow region near the anode and much of the Hall field recovery occurs in the downstream region. Using the averaged Hall current density $<j_r>$, Hall field $<E_r>$, and estimated electron temperature, the effective values of the electrical conductivity and Hall parameter are calculated as follows:

$$\sigma_{\text{eff}} = \frac{1}{U^2B^2}\left[\frac{<j_r>^2}{<\text{LOSS}>}(<E_r>^2 + U^2B^2)\right.$$

$$\left. + <\text{LOSS}> - 2<E_r><j_r>\right] \quad (1)$$

$$\beta_{\text{eff}} = \frac{<j_r>}{UB<\text{LOSS}>}[<E_r>^2 + U^2B^2] - \frac{<E_r>}{UB} \quad (2)$$

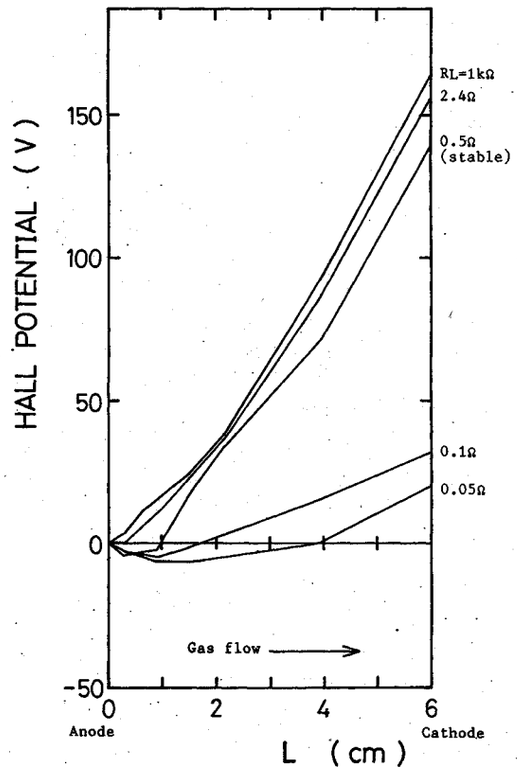

Fig. 6 Hall potential distributions along the flow direction.

where $<\text{LOSS}>$ denotes the energy loss of electrons due to elastic collision and radiation, and this can be calculated on the basis of electron temperature.[12]

The estimated effective electrical conductivity and effective Hall parameter are 197 S/m and 7.1, respectively. A recovery of 85 and 90% of each of their respective ideal values could be achieved for load resistance of 0.5 Ω.

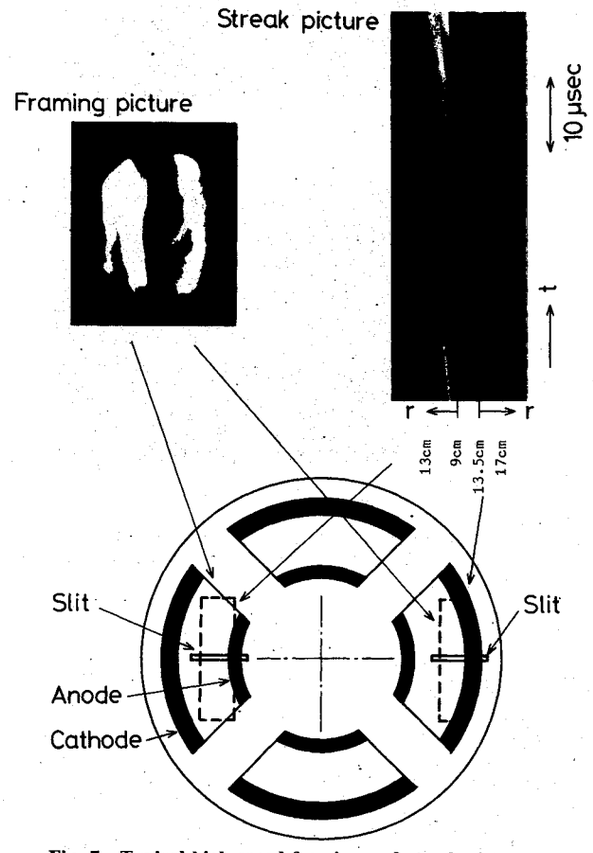

Fig. 7 Typical high-speed framing and streak pictures.

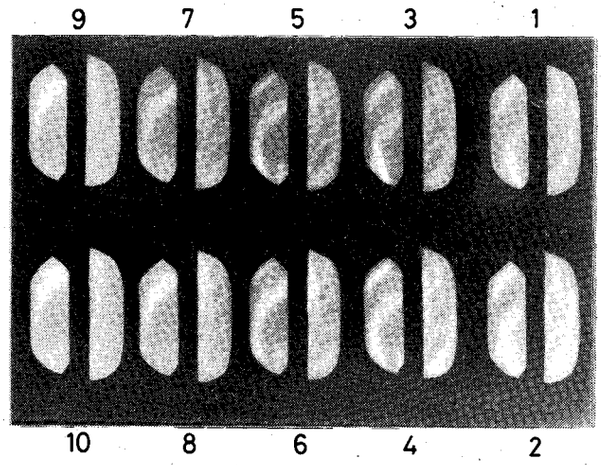

Fig. 8 High-speed framing pictures for $R_L = 0.05$ Ω.

Discharge Structure in the Disk Channel

High-speed framing and streak photography technique was adopted to study the discharge structure in the disk channel. Figure 7 shows the typical framing and streak photoghraphs. The disk walls are provided with two windows through which to observe the discharge. The left side of a frame shows the inlet region ($9 < r < 13$ cm) of the disk channel and the right one shows the region downstream ($13.5 < r < 17$ cm), so that a part of both the anode and cathode surfaces can be observed. An investigation of high-speed photographs does not indicate any strong arc spot on the surface of either electrode. At the time of taking the streak pictures, the image of the slit at the disk channel is positioned along the flow direction and, therefore, the streak pictures show the motion of the discharge along the radial direction. Plasma luminosity decreases with the radial distance because of the decrease in the channel width along the radial direction.

Figures 8 and 9 show the framing and the streak pictures, respectively. Also shown in Fig. 9 is the trace of Hall field measured at $r = 15$ cm for the load resistance of 0.05 Ω, where the plasma is in the partially ionized potassium regime. We can see from the framing pictures (Fig. 8) that the discharge is strongly inhomogeneous, especially near the anode where it has intense spiral arcs with fine structures. The observed discharge structure agrees well with that observed in the generator operated with unstable plasma.[4,17] It can also be seen that this inhomogeneous discharge moves downstream, causing the fluctuation in the Hall field and resonance line intensity.

A detailed study of the streak pictures leads to an understanding that a few intense discharges move downstream and that this unsteady motion of discharges is confined to the region between the anode and the center of the channel. This region coincides with the negative potential region of the Hall potential distribution for the case of $R_L = 0.05$ Ω in Fig. 6.

The framing pictures are shown in Fig. 10 and the streak pictures in Fig. 11; the trace of the Hall field for the load resistance of 0.5 Ω. It must be noted that with this external load, the plasma is in the regime of fully ionized seed. In such circumstances, a bright and uniform discharge is achieved (ex-

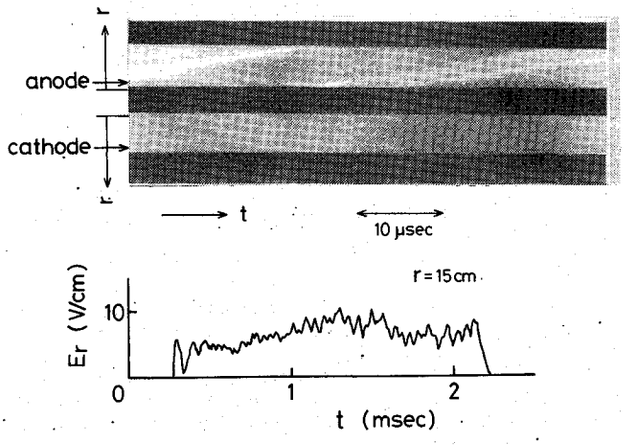

Fig. 9 High-speed streak pictures and trace of Hall field for $R_L = 0.05$ Ω.

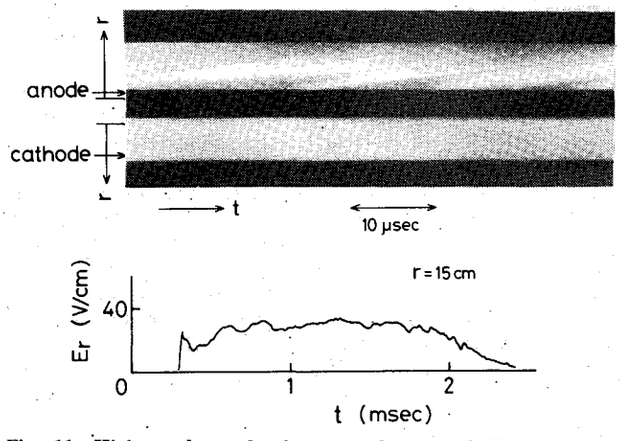

Fig. 11 High-speed streak pictures and trace of Hall field for $R_L = 0.5$ Ω.

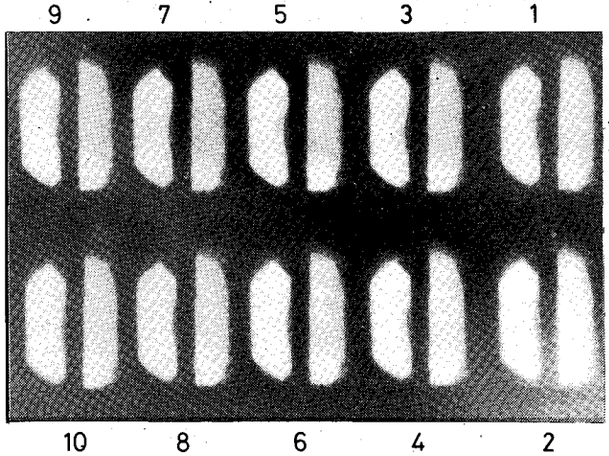

Fig. 10 High-speed framing pictures for $R_L = 0.5$ Ω.

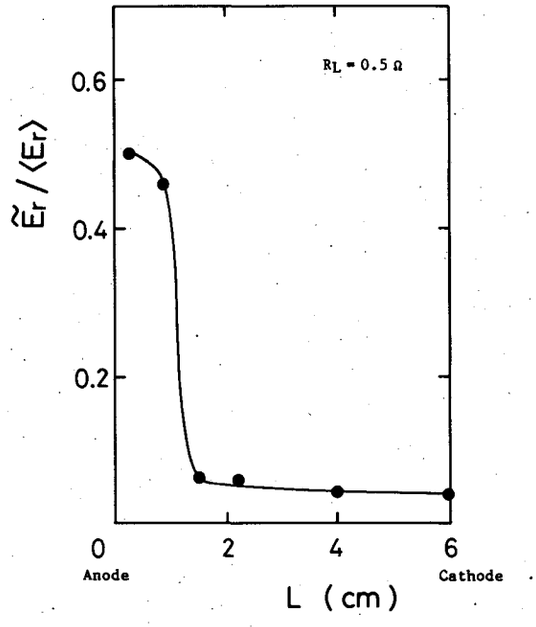

Fig. 12 Variation of fluctuation level of Hall field along the flow direction for $R_L = 0.5$ Ω.

cept in the narrow region near the anode) and the fluctuation of Hall field almost disappears. The streak pictures show that the intense discharges move downstream with increasing width and decreasing intensity. The number of intense discharges increases when compared to those for the unstable condition (see Fig. 9). The region of the nonuniform and unsteady discharge is confined to a range of about 2 cm from the anode and this range almost coincides with the length of negative potential region for the case of $R_L = 0.5\ \Omega$ in Fig. 6. This is also assured by the results of the variation of the fluctuation level in Hall field along the flow direction as shown in Fig. 12. As can be seen, the fluctuation level is high in the entrance relaxation region, but decreases rapidly in the region downstream. It has to be noted that the unsteady and nonuniform discharge in the entrance region tends to be uniform downstream. This result agrees well with that of the numerical analysis reported in Ref. 18, where a potential drop in the entrance region of the channel had occurred under the conditions where finally the fully ionized seed could be achieved.

Conclusions

The experimental results reported here on the discharge phenomena in nonequilibrium MHD disk generator lead to the following conclusions:

1) An unsteady motion of strongly constricted discharge with a high fluctuation level in entrance region has been found. This region of unsteady motion almost coincides with the negative Hall potential region.

2) For the load condition corresponding to complete seed ionization, a uniform discharge is achieved at the downstream region, whereas a strongly inhomogeneous and unsteady discharge is confined to the entrance region.

3) On the other hand, for the load condition corresponding to an unstable plasma, it is observed that the downstream movement of an intense spiral arc causes fluctuation in the plasma in the downstream portion.

Acknowledgment

The authors wish to express their grateful thanks to Mr. D. Biswas for useful discussion. This research was supported partially by a Grant in Aid for Energy Research from the Japan Ministry of Education.

References

[1]Rosa, R. J., *Magnetohydrodynamic Energy Conversion*, McGraw-Hill Book Co., New York, 1958, Chaps. 4 and 5.

[2]Mitchner, M. and Kruger, C. H., *Partially Ionized Gases,* John Wiley & Sons, New York, 1973, Chap. 4.

[3]Loubsky, W. J., Hruby, V. J., and Louis, J. F., "Detailed Studies in a Disk Generator with Inlet Swirl Driven by Argon," *Proceedings of 15th Symposium on Engineering Aspects of MHD*, May 1976, pp. VI.4.1-VI.4.5.

[4]Sens, A.F.C., Veefkind, A., Uhlenbusch, J.F. and Rietjens, L.H.Th., "Experimental Studies on a Closed Cycle MHD Disk Generator," *Proceedings of 8th International Conference on MHD Electrical Power Generation,* Sept. 1983, pp. M.11.1-M.11.9.

[5]Brederlow, G. and Hodgson, R.T., "Electrical Conductivity in Seeded Noble Gas Plasmas in Crossed Electric and Magnetic Fields," *AIAA Journal*, Vol. 6, July 1968, pp. 1277-1284.

[6]Kerrebrock, J.L. and Dethlefsen, R., "Experimental Investigation of Fluctuations in a Nonequilbrium MHD Plasma," *AIAA Journal,* Vol. 6, Nov. 1968, pp. 2115-2121.

[7]Zauderer, B., "Discharge Structure and Stability of a Nonequilibrium Plasma in a Magnetohydrodynamic Channel," *The Physics of Fluid,* Vol. 11, Dec. 1968, pp. 2577-2585.

[8]Gilpin, R. R. and Zukoski, E. E., "Experimental and Theoretical Studies of Electrothermal Waves," *AIAA Journal*, Vol. 7, Aug. 1968, pp. 1438-1445.

[9]Velikhov, E. P. and Dykhne, A. M., "Plasma Turbulence Due to the Ionization Instability in a Strong Magnetic Field," *Proceedings of 6th International Conference on Ionization Phenomena in Gases,* 1963, pp. 511-512.

[10]Kerrebrock, J. L., "Nonequilbrium Ionization Due to Electron Heating: I. Theory," *AIAA Journal*, Vol. 2, June 1964, pp. 1072-1080.

[11]Nakamura, T. and Riedmüller, W., "Stability of Nonequilbrium MHD Plasma in the Regime of Fully Ionized Seed," *AIAA Journal*, Vol. 12, May 1974, pp. 661-668.

[12]Tong, J. Z. et al., "Electrical Discharge in a Nonequilibrium Slightly Seeded MHD Plasma," *Energy Conversions and Management*, Vol. 23, No. 1, 1983, pp. 11-21.

[13]Yamasaki, H. and Shioda, S., "MHD Power Generator With Fully Ionized Seed," *Journal of Energy*, Vol. 1, 1977, pp. 301-305.

[14]Yamasaki, H., Masuhara, Y. and Shioda, S., "Experimental Studies of a Linear MHD Generator with Fully Ionized Seed," *Journal of Energy*, Vol. 2, Nov.-Dec. 1978, pp. 337-341.

[15]Shioda, S. et al., "Power Generation Experiments and Prospects of Closed Cycle MHD with Fully Ionized Seed," *Proceedings of 7th International Conference on MHD Electrical Power Generation*, Vol. 2, 1980, pp. 685-695.

[16]Harada, N. et al., "Effect of Ionization Relaxation and Potential Drop near Electrodes on Fully Ionized Seed Closed Cycle MHD Generators," *Proceedings of 8th International Conference on MHD Electrical Power Generation,* Sept. 1983, pp. M.13.1-M.13.4.

[17]Sens, A. F. C., Veefkind, A., Uhlenbuch, J. F., and Rietjens, L. H. Th., "First Experimental Results with the Eindhoven Shock Tube-Driven Closed Cycle MHD Disk Generator," *Proceedings of 20th Symposium on Engineering Aspects of MHD*, 1982.

[18]Kabashima, S., Yoshikawa, Y., Yamasaki, H., Harada, N., and Shioda, S., "Dynamical Behavior of Disk Type Closed Cycle MHD Generator," *Proceedings of 21st Symposium on Engineering Aspects of MHD*, 1983, pp. 6.3.1-6.3.8.